

Raman spectroscopic detection of physiology changes in plasmid-bearing *Escherichia coli* with and without antibiotic treatment

Angela Walter · Martin Reinicke · Thomas Bocklitz ·
Wilm Schumacher · Petra Rösch · Erika Kothe ·
Jürgen Popp

Received: 13 December 2010 / Revised: 28 January 2011 / Accepted: 16 February 2011 / Published online: 20 March 2011
© Springer-Verlag 2011

Abstract Bacterial resistances against antibiotics are increasingly problematic for medical treatment of pathogenic bacteria, e.g., in hospitals. Resistances are, among other genes, often encoded on plasmids which can be transmitted between bacteria not only within one species, but also between different species, genera, and families. The plasmid pDrive is transformed into bacteria of the model strain *Escherichia coli* DH5 α . Within this investigation, we applied micro-Raman spectroscopy with two different excitation wavelengths in combination with support vector machine (SVM) and linear discriminant analysis (LDA) to differentiate between bacterial cultures according to their cultural plasmid content. Recognition rates of about 92% and 90% are achieved by Raman excitation at 532 and 244 nm, respectively. The SVM loadings reveal that the pDrive transformed bacterial cultures exhibit a higher DNA content

compared to the untransformed cultures. To elucidate the influence of the antibiotic, ampicillin-treated cultures are also comprised within this study and are classified with rates of about 97% and 100% for 532 and 244 nm Raman excitation, respectively. The Raman spectra recorded with 532 nm excitation wavelength show differences of the secondary protein structure and enhanced stress-related respiration rates for the ampicillin-treated cultures. Independent cultural replicates of either ampicillin-challenged or non-challenged cultures are successfully identified with identification rates of over 90%.

Keywords Raman spectroscopy · Antibiotic resistance · Plasmids

Published in the special issue *Biophotonics* with Guest Editors Jürgen Popp and Reiner Salzer.

Electronic supplementary material The online version of this article (doi:10.1007/s00216-011-4819-4) contains supplementary material, which is available to authorized users.

A. Walter · T. Bocklitz · W. Schumacher · P. Rösch · J. Popp (✉)
Institut für Physikalische Chemie, Friedrich-Schiller-Universität,
Helmholtzweg 4,
07743 Jena, Germany
e-mail: juergen.popp@uni-jena.de

M. Reinicke · E. Kothe
Institut für Mikrobiologie, Friedrich-Schiller-Universität,
Neugasse 25,
07743 Jena, Germany

J. Popp
Institut für Photonische Technologien,
Albert-Einstein-Strasse 9,
07745 Jena, Germany

Introduction

Plasmids are extra-chromosomal DNA elements which may be transmitted by conjugation from one bacterium to another and which encode potentially useful traits [1]. Thus, plasmids have been used to construct vectors for biotechnology, including also systems in which conjugative transfer is used to introduce DNA into an organism of a different domain [2]. In order to select transformed cells, antibiotic resistance genes are usually encoded on the plasmid.

Plasmid isolation and sequencing are standard molecular biology techniques that require cultivation of pure strains. The DNA is extracted, via an extensive sample preparation, from the pure cultures for DNA sequencing [3]. However, polymerase chain reaction approaches and metagenomics allow for the investigation of native communities, but require experienced personal [4, 5]. In order to additionally

achieve physiological characterization of the bacteria concerning, e.g., the protein structure, enzyme pattern, lipid content, or cell wall composition, further analytical methods are required, including also isolation and purification steps [6–10].

To retrieve both, the genetic as well as the physiological information, vibrational spectroscopy is applied providing complex spectral fingerprints and requiring simple sample preparation. Therefore, vibrational spectroscopic approaches have successfully emerged as an important tool in biosciences [11, 12]. Raman spectroscopy, as one vibrational spectroscopic technique, excels by the advantage to manipulate the features present in the spectral fingerprint by choosing specific excitation wavelengths [13]. Hence, investigation of complex systems like an entire microorganism can be simplified. For example, applying UV-resonance Raman spectroscopy results in DNA and protein enhanced signals in the spectrum. The excitation within the visible wavenumber region at, e.g., 532 nm enhances cytochrome bands [14] and reflects all other cell components like proteins, lipids, polysaccharides, DNA and the spore component Ca-dipicolinate [15, 16], instead. So, Raman spectroscopy in combination with statistical analysis can be used to rapidly differentiate and identify, e.g., bacteria using excitation wavelengths within the visible [17–22] and the UV region [23, 24]. Besides the bacteria identification on strain and species level, also spectral changes induced by antibiotic treatment have been investigated by Raman spectroscopy [25–28]. However, none of these investigations concern plasmid-transferred antibiotic resistances only the secondary structure of the isolated plasmid pUC19 from *Escherichia coli* (*E. coli*) has been studied by means of Raman spectroscopy before [29].

Since antibiotic resistances of bacteria are of paramount importance, fast and reliable detection is required. Furthermore, it would be helpful, if the resistance potential of a bacterium carrying certain plasmids can be detected before the antibiotic resistance is activated.

This paper aims for the detection of transient plasmids as a source of antibiotic resistance genes as well as the cellular response to antibiotic-induced selective pressure by applying the combination of Raman spectroscopy and chemometric analysis. The Raman excitation wavelengths at 532 and 244 nm are chosen to record the genetic- and physiological-related spectra.

Firstly, the differentiation of *E. coli* bacteria according to their plasmid content in the absence of antibiotic-induced pressure will be tested to clarify if Raman spectroscopy is capable to detect plasmids within bacterial cells. The transformed (+plasmid pDrive) bacterial cells contain a different DNA content compared to the untransformed cells induced by the high copy number of the plasmid. The transformed and non-transformed bacterial cultures will be

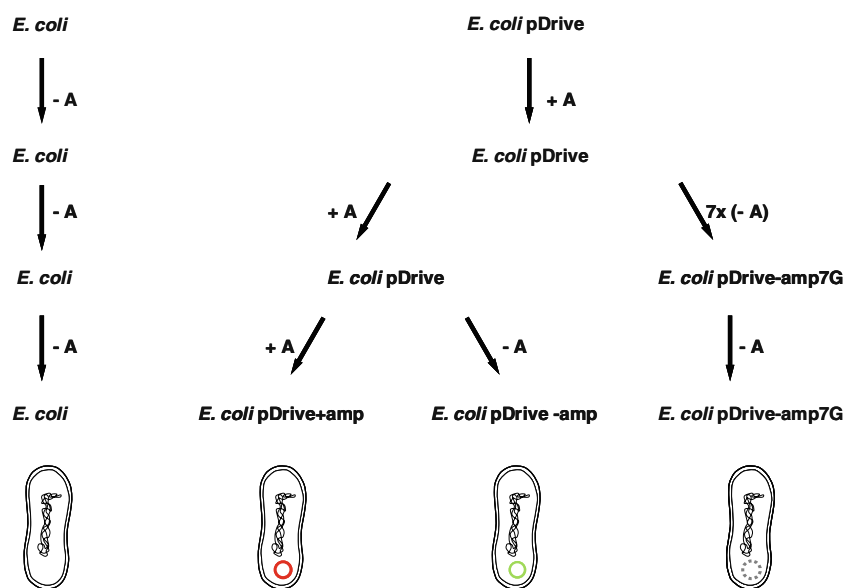
classified by the application of support vector machine (SVM). SVM is a very powerful statistical tool for differentiating between several classes and additionally reveals the Raman signals that have a strong impact on the classification. Secondly, we will discuss the spectral impact of the down-regulated plasmid content regulated by several cultivation steps without selective pressure. A transformed bacterial culture which is cultivated without selective pressure results in mixed cultures plasmid-containing and plasmid-free cells, since the latter ones are also able to grow. The transformed bacteria are cultured either under challenged (with ampicillin) or non-challenged conditions (after one and seven cultivation steps without ampicillin). The relation of these four bacterial classes will be evaluated by using linear discriminant analysis (LDA). LDA scoreplots of multi-class problems are more easily accessible compared to the corresponding SVM scoreplots. Thirdly, the influence of the antibiotic on the *E. coli* cells will be analyzed by using SVM to estimate the potential of Raman spectroscopy to distinguish between cultures that have been incubated in media with and without ampicillin. Additionally, biologically independent replicates of these two bacterial classes will be identified.

Experimental section

Sample preparation The investigation was carried out on the model system *E. coli* DH5 α [30] grown in Standard I media 25 g/L agar (Merck, Darmstadt, Germany) with or without 100 μ g/ml ampicillin. Competent *E. coli* DH5 α were transformed with plasmid pDrive (Qiagen, Hilden, Germany) using standard protocols [31]. The plasmid pDrive encodes antibiotic resistances against ampicillin and kanamycin. Cultivation was performed in four to six different, biologically independent replicates for each sample. The bacterial cell of the cultures without and with plasmid grown in the presence and absence of ampicillin (see Fig. 1 for experimental setup) were harvested from the exponential growth phase. The collected biomass was washed six times with distilled water and then loaded on several fused silica objective slides and dried. Spectra were recorded using excitation wavelengths of 532 and 244 nm for each biological replicate from two to five slides, the exact numbers are summarized in Table 1 for all strains.

Raman spectroscopy Micro-Raman spectra were recorded using 532 nm as an excitation wavelength from a frequency doubled Nd:YAG-Laser (Coherent, Dieburg, Germany). An inverse Raman setup (HR Labram invers; Jobin Yvon, Horiba) with a focal length of 800 mm was combined with a 300 lines/mm grating. With a $\times 100$ microscope objective (PL Fluotar L100x/0.75; Leica) of 1 mm working distance,

Fig. 1 Experimental design of this study including all cultivation steps, depicted by the arrows, with the standard media and with ampicillin (+A) and without ampicillin (-A). The different colors signify the investigated cultures: *E. coli* (black), *E. coli* pDrive+amp (red), *E. coli* pDrive-amp (green) and *E. coli* pDrive-amp7G (gray)



the laser beam was focused on the sample with an approximated focus of about 1 μm , the net power was 5 mW and the spectral resolution was about 10 cm^{-1} . The detector was a Peletier cooled and back-illuminated CCD camera (1024 \times 512 pixel).

The UV-resonance Raman spectroscopy was performed using an HR micro-Raman setup (HR800 LabRam, Jobin Yvon, Horiba) with a focal length of 800 mm and combined with a 2400 lines/mm grating. As an excitation wavelength, the 244 nm-line from an intracavity frequency doubled argon ion laser (Innova300-MotoFreD, Coherent Inc.) was used that deliver slightly less than 1 mW at the sample. The laser was focused on the sample by a $\times 40$ UV achromatic fused-silica-CaF₂ microscope objective (LMU-40-UVB, NA 0.5) with broadband UVB coating. The CCD-detector is liquid N₂-cooled and the spectral resolution was 5 cm^{-1} . For the UV-resonance Raman spectra the objective slide was rotated during the measurements with 6 rpm and moved manually twice for each rotation to avoid the spectral recording from one circle only. All Raman spectra were integrated for 60 s.

Data preprocessing and chemometrical methods The data preprocessing and the chemometrical analysis was processed in the statistical language R [32]. For data

preprocessing, internal wavenumber calibration was carried out orientating on pre-selected sharp peaks, present in all spectra and covering the spectral region of interest (244 nm: 782 \pm 10, 1009 \pm 10, 1174 \pm 8, 1480 \pm 10 and 1614 \pm 10 cm^{-1} ; 532 nm: 781 \pm 10, 1001 \pm 10, 1125 \pm 8, 1446 \pm 10, 1658 \pm 10 and 2935 \pm 20 cm^{-1}). New supporting points were defined at every wavenumber point between 630 and 1735 cm^{-1} for UVRR spectra and at every third wavenumber point between 500 and 3200 cm^{-1} for spectra recorded using 532 nm excitation. Baseline correction with a sensitive nonlinear iterative peak clipping (SNIP) algorithm [33] was applied of second- and fourth-order clipping filter for the spectra recorded using the wavelengths of 244 and 532 nm, respectively. For the evaluation and identification of the UVRR spectra concerning the classification only spectra without cosmic spikes were used and the entire spectra were included. The spectra recorded using the excitation wavelengths of 532 nm were reduced within the fingerprint region from 650 to 1703 cm^{-1} and the CH stretching region from 2831 to 3017 cm^{-1} . These wavenumber regions are defined by the position of relevant Raman signals. All spectra were vector normalized. For smoothing and dimension reduction of the spectra, a principal component analysis (PCA) was performed. To avoid overfitting, the first ten principal components were introduced to the chemometrical analysis. The exact number 10 was determined by the most

Table 1 Number of spectra per replicate for the two datasets: recorded using the excitation wavelength at 244 nm and 532 nm for all four strains

Excitation wavelength	244 nm					532 nm							
	1	2	3	4	5	6	7	8	1	2	3	4	5
<i>E. coli</i>	6	6	7	8	5	5	–	–	13	38	29	14	30
<i>E. coli</i> pDrive-amp	8	6	10	3	–	–	–	–	17	43	29	30	–
<i>E. coli</i> pDrive-amp7G	8	3	4	4	4	–	–	–	23	26	23	13	–
<i>E. coli</i> pDrive+amp	4	7	3	3	18	15	14	7	13	26	27	22	27

successful classification results and contain for each classification task over 99.8% of the total variance of the dataset. For classification and identification, LDA [34] and SVM [35, 36] were applied. For the application of the SVM, the implementation of Chang et al. [37] was used with a linear kernel and a tenfold cross validation for model evaluation, whereas the dataset is randomly split.

Results and discussion

Discrimination of plasmid-bearing cultures from non-transformed E. coli cultures *E. coli* transformed with the high copy number plasmid pDrive is capable to resist selective pressure induced by ampicillin due to β -lactamase expression. The pDrive carrying *E. coli* cultures have either been incubated in medium with (+amp; red) or without ampicillin for one (-amp; green) or seven (-amp7G; gray) culture transfers (see Fig. 1). In addition, a culture was used which had been grown without selective pressure for seven culture transfers (*E. coli* pDrive-amp7G; gray) which has potentially led to a loss of plasmid in some bacteria resulting in a mixed culture of *E. coli* and *E. coli* pDrive bacteria. Non-transformed (*E. coli*) and transformed cultures incubated without the antibiotic (*E. coli* pDrive-amp) are compared according to the DNA content. Furthermore, transformed cells grown only one step of cultivation without the antibiotic and are compared to those cells incubated seven cultivation steps without antibiotic to record the change in the culture composition. The cultures were sampled from the exponential phase (see Electronic Supplementary Material Fig. S1). In both investigations, the antibiotic thus had no direct impact on the cells, and differences to untransformed *E. coli* are due to the presence of the additional plasmid DNA and its expression. The high copy number plasmid pDrive has a size of 3.85 kb and is replicated to around 80 copies per cell. The genomic DNA consists of 4.64 Mb for *E. coli*, leading to about 7.5% of cellular DNA in a transformed cell being plasmid-derived.

The success of the transformation was checked by plating on ampicillin-containing media. Colonies from these plates were used for further cultivation. The untransformed strain was sensitive to ampicillin. The experiment requires an estimation of cell numbers that contained the plasmids even under non-selective conditions. The growth of the bacterial cultures was tested under both, selective (ampicillin-containing standard medium) and non-selective (standard medium), conditions. Comparing the colony forming units (cfu) under selective and non-selective growth conditions results in 10% to 19% cultural growth on the antibiotic containing medium after one cultivation step without

ampicillin (*E. coli* pDrive-amp). The *E. coli* pDrive-amp7G cultures, cultivated for seven culture cycles without ampicillin, showed only 0.1% to 0.2% cultural growths on the antibiotic containing medium. Therefore, part of the culture exhibited the phenotype of plasmid-containing *E. coli*, while the majority had lost the plasmid required to resist the antibiotic at the time of sampling. This effect is, as expected, more increased for the *E. coli* pDrive-amp7G cultures, and therefore, results in mixed culture composed of cells with and without plasmids for both cultivation types. Due to the culture characteristics, bulk Raman measurements are required to ensure that the bacteria within the laser focus represent the analyzed culture.

The Raman spectra recorded using 244 and 532 nm as excitation wavelengths for all four bacterial cultures (*E. coli*: black; *E. coli* pDrive-amp: green; *E. coli* pDrive-7amp: gray and *E. coli* pDrive+amp: red) are presented in Fig. S2 (Electronic Supplementary Material). For both excitation wavelengths, representative raw-spectra as well as the averaged preprocessed spectra are shown. Additionally, the peak positions of the most prominent bands are denoted within the spectra and the band assignment corresponding to previously published studies [15, 19, 27, 38–40] is summarized in Table S1 (Electronic Supplementary Material). The following discussions of the discriminating vectors are based on this band assignment but include further literature [39, 41, 42] for a more detailed interpretation. Raman excitation at 244 nm enhances specifically DNA and protein signals, whereas excitation at 532 nm results in additional spectral signals like carbohydrates and lipid bands, representing the physiological status of the cell.

In the following, the differences of DNA content detected via Raman spectroscopy will be discussed and linked to cellular changes. Figure 2 contains the SVM classification of *E. coli* pDrive-amp (green) and *E. coli* (black) spectra recorded using an excitation wavelength at 244 and 532 nm, respectively. Panel A shows the scoreplots of the support vectors versus the spectrum number, with lower spectrum numbers for the pDrive-amp culture (green circles) and higher spectrum numbers for the *E. coli* spectra (black circles). The separation of these two classes is indicated by the gray dotted line. *E. coli* and pDrive-amp cultures are classified by SVM with accuracies of $89.5 \pm 15.3\%$ and $92.2 \pm 5.4\%$ for the spectra recorded with an excitation wavelength of 244 and 532 nm, respectively. Panel B of Fig. 2 contains the preprocessed and averaged Raman spectra of the *E. coli* (black) and pDrive-amp cultures (green). Here, we concentrate on the spectral differences showing up in the difference spectrum (red spectrum) of the class mean spectra and the discriminating vector (see lower part of the spectrum in Fig. 2b) comprising the separation features of the classes. The

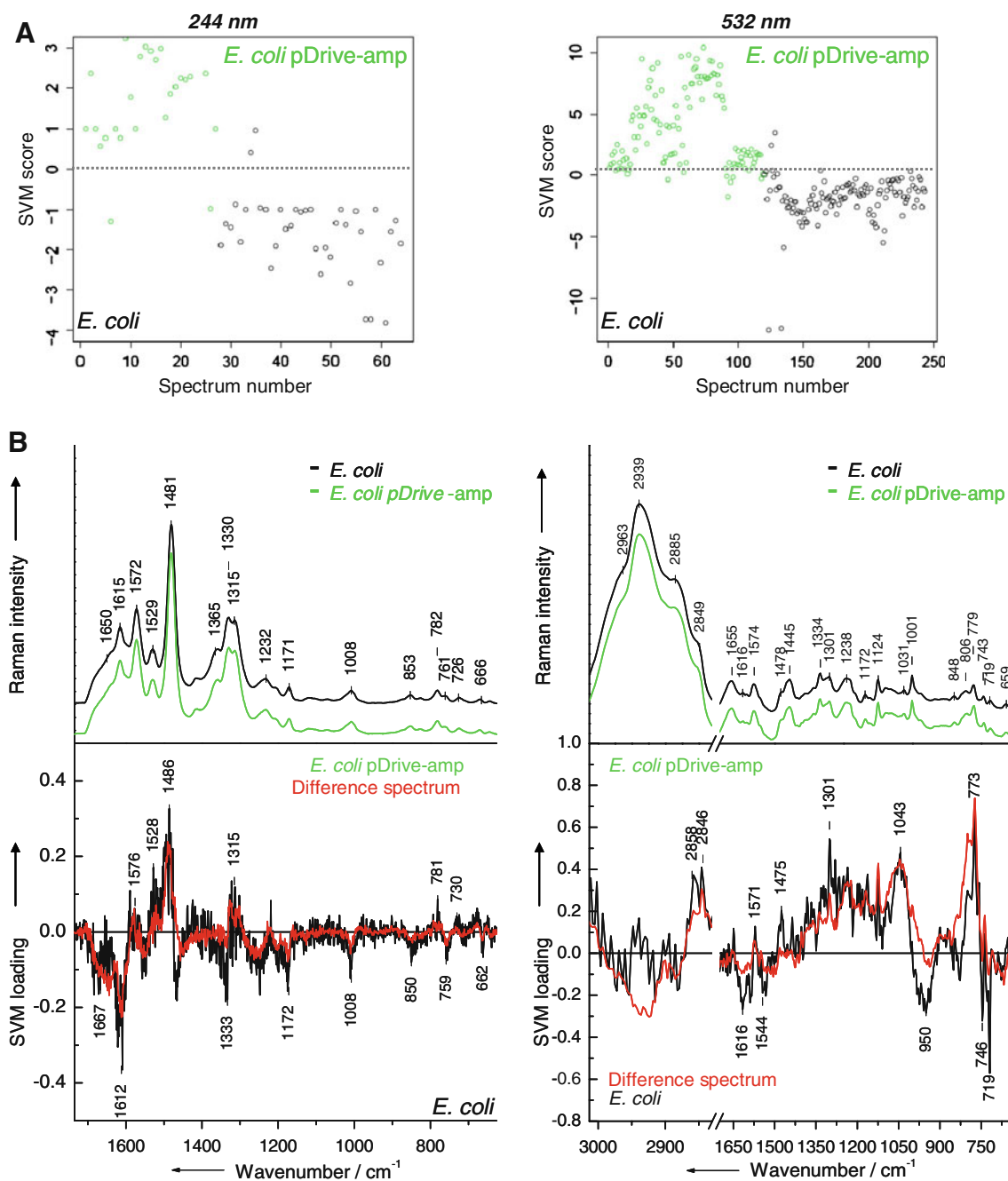


Fig. 2 Classification of cells with and without pDrive grown under non-selective conditions. **a** SVM scoreplots of *E. coli* (black) and *E. coli* pDrive-amp (green) spectra recorded with Raman excitation wave-

lengths at 244 (left) and 532 nm (right). **b** Corresponding preprocessed and averaged Raman spectra, the difference spectra of the class mean spectra and the discriminating SVM vectors (SVM loadings)

spectral features that are present in the difference spectrum show high similarities with the support loadings. Therefore, it can be assumed that the signals of the support loadings can be interpreted as most important for the discrimination of the two classes. This is the case for all the following examples we will discuss within this study. Support loadings contain positive and negative peaks correlating with characteristics of the spectra with positive and negative scores. As can be seen from the scoreplots

(Fig. 2a), plasmid-containing cultures (*E. coli* pDrive-amp) excited at both wavelengths exhibit positive scores. Therefore, the positive peaks of the support loadings characterize the peaks which exhibit a relatively higher intensity in the *E. coli* pDrive-amp spectra compared to the *E. coli* spectra. In the following, only Raman signals of the discriminating vectors will be discussed which support directly microbiological findings. Microorganisms exhibit a complex substance composition and the recorded

Raman spectra are a superposition of the Raman spectra originating from the individual components. Therefore, most Raman signals of bacterial spectra are due to vibrations of several cell components. Thus, the discriminating vector can contain signals which correlate to band shoulders within the Raman spectra, but do not exhibit an individual peak at that position.

The discriminating vector of the classification of the UVRR spectra comprises six positive signals located at 1576, 1528, 1486, 1315, 781, and 730 cm^{-1} which are assigned to DNA vibrations with some deviation to the peak position in the Raman spectra due to the low signal to noise ratio of the discriminating vector. The discriminating vector contains six negative signals located at 1667, 1612, 1172, 1008, 850 and 759 cm^{-1} originating from protein vibrations. DNA vibrations contribute to the bands appearing at 1333 and 662 cm^{-1} .

The discriminating vector derived from classification of the spectra recorded with 532 nm as excitation wavelength exhibits positive signals at 2858 and 2846 cm^{-1} which occur as a shoulder of the CH stretching vibration at 2939 cm^{-1} in the Raman spectra and are assigned to lipid vibrations. The positive signals at 1571, 1475 and 773 cm^{-1} are assigned to DNA and RNA vibrations. The discriminating vector contains two signals that are located at 1301 and 1043 cm^{-1} and can tentatively be assigned to lipid and carbohydrate vibrations, respectively. Protein vibrations contribute to the negative signals located at 1616, 1544 and 950 cm^{-1} , whereas the last one additionally originates from polysaccharide vibrations. The Raman band at 719 cm^{-1} is due to an adenine vibration and the one at 746 cm^{-1} can be assigned to cytochrome vibrations. Cytochrome generally generates three marker bands in the Raman spectrum recorded with an excitation wavelength at 532 nm. Besides the signal at 746 cm^{-1} , the other two bands arise in spectral regions where additional signals appear and are probably superposed by those within the SVM discriminating vector.

The discriminating vectors reveal for the Raman spectra recorded with both excitation wavelengths that the classifications of *E. coli* and *E. coli* pDrive-amp cultures are based on a higher ratio of DNA to protein content of the transformants and higher ratio of protein to DNA content for the non-transformed strain. Raman excitation at 532 nm also reveals a strong discriminating influence of the RNA content, which is increased in the *E. coli* pDrive-amp cultures. Additional physiological information is retrieved from the spectra excited in the visible wavenumber region. Here, higher lipid content can be found for the transformant cultures, whereas non-transformed cultures exhibited higher cytochrome content.

Comparison of ampicillin-treated cultures with E. coli pDrive-amp and untransformed cultures Transformed

cells have no need to express the plasmid-contained information if there is no selective pressure. In the following, cultures of *E. coli* pDrive grown without and with ampicillin are compared. The plasmid-encoded resistance mechanism against ampicillin is based on β -lactamase production, which has an influence on the overall substance composition of the cells. The enzyme β -lactamase cleaves the β -lactam-ring of ampicillin. [43, 44] By plating, we found (see above) that 80% of the cells from the *E. coli* pDrive-amp cultures did not grow on ampicillin-containing media. Thus, the loss of plasmid was increased by seven repetitive cultivation steps without ampicillin. The resulting *E. coli* pDrive-amp7G showed 0.1% to 0.2% of cfu on ampicillin-containing medium as compared to media without ampicillin, showing the expected loss of plasmid. To further elucidate whether this aspect has an influence on classification and identification concerning antibiotic, challenged *E. coli* pDrive-amp7G are included in the following discussion.

Figure 3a and b show the scoreplots with score 1 versus score 2 resulting from the LDA using the formerly introduced color coding. The ellipses within the LDA scoreplots illustrate the distribution of the group members via the doubled standard deviation with at least 87% probability. Here, the *E. coli* pDrive+amp cultures (red) are clearly separated in both plots and will be discussed separately. As already shown in Fig. 2, for which SVM was applied, *E. coli* (black) and pDrive-amp (green) are clearly separated from each other. LDA evaluation of both Raman excitation wavelengths results in different distributions of the *E. coli* pDrive-amp7G spectra (gray) compared to the pDrive-amp (green) and *E. coli* (black) cultures. For UVRR spectra, the pDrive-amp7G cultures overlap with both, the *E. coli* (black) and the pDrive-amp (green) cultures. Since the *E. coli* pDrive-amp7G cultures showed massive plasmid loss as confirmed by plating, their DNA content is expected to be between the cultural DNA content of *E. coli* and pDrive-amp cultures. The LDA scoreplot derived from spectra using the DNA enhancing excitation wavelength (244 nm) supports these expectations.

The impact on physiology is more significant in Raman spectra recorded with an excitation wavelength at 532 nm compared to UV RR spectra. In the scoreplots of the Raman spectra excited at 532 nm, the scores of the *E. coli* pDrive-amp7G spectra completely coincide with the scores of the *E. coli* pDrive-amp spectra. This supports the idea of lower plasmid content in conjunction with a lack of expression of plasmid-encoded genes due to one or more cultivation steps without selective pressure.

Influence of the antibiotic The LDA scoreplots of Fig. 3a and b also contain the distributions of the scores from the *E. coli* pDrive+amp (red) spectra. The analysis of the Raman spectra recorded using the excitation wavelengths at

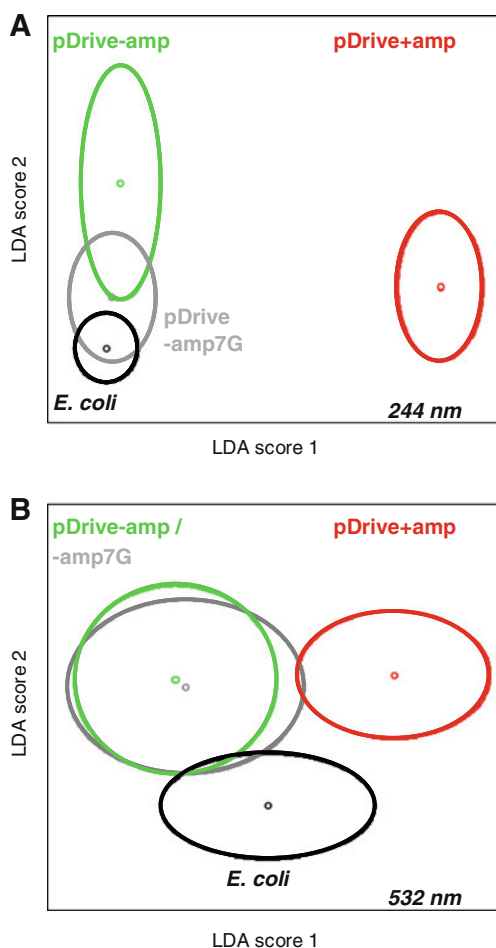


Fig. 3 Scoreplots of the LDA applied to the Raman spectra recorded using the excitation wavelengths of 244 nm (a) and 532 nm (b) of *E. coli* (black), *E. coli* pDrive-amp (green), *E. coli* pDrive-amp7G (gray) and *E. coli* pDrive+amp (red) cultures. Ellipsoids depict the distribution of the group members via doubled standard deviation

244 and 532 nm show clear separation of this cultural class from the other three classes. Thus, the presence of ampicillin and its impact on the bacterial cell has a discriminating influence on the spectral classification. To investigate the influence of the antibiotic on this separation, the four-class problem comparing all four different bacterial classes is reduced to a two-class dataset containing ampicillin-challenged (*E. coli* pDrive+amp) and non-challenged bacteria (*E. coli*, *E. coli* pDrive-amp and *E. coli* pDrive-amp7G). For both excitation wavelengths, the correlating SVM scoreplots are depicted in Fig. 4a. The non-challenged bacteria are represented by black circles, the bacteria cultivated with ampicillin by red circles and the gray dotted line separates these two classes. The evaluation accuracy of the SVM is 100% and (96.9±2.8)% for the spectra recorded with an excitation wavelength of 244 and 532 nm, respectively.

Figure 4b contains the preprocessed and averaged Raman spectra recorded with excitation wavelengths of 244 and 532 nm as well as the discriminating vectors correlating with the SVM scoreplots depicted in Fig. 4a. The discriminating vector corresponding to the separation accomplished with the UVRR spectra exhibits the most intense positive signals at 1651 cm^{-1} which is assigned to the amid I vibration of proteins. Further protein vibrations present in the discriminating vector are the signals at 1170, 851, and 761 cm^{-1} exhibiting slight variations to the signals within the averaged Raman spectra. Besides the protein vibrations, DNA / RNA vibrations are also present in the discriminating vector observable at 1524, 1309, 782, 723, and 671 cm^{-1} . The negative signals of the discriminating support vector correspond to the challenged cultures, and therefore, to the impact of the ampicillin. The influence of ampicillin is manifesting itself as changes within the band profiles. The signals located at 1559, 1492, 1469, and 1345 cm^{-1} could be interpreted as variations of nucleotides G+A vibrations located at 1572, 1481, and 1330 cm^{-1} in the original UVRR spectra. The signal at 1377 cm^{-1} is most likely correlated to the band at 1365 cm^{-1} , assigned to superimposed nucleic acid and protein vibration. The signal located at 1618 cm^{-1} is assigned to a signal in the UVRR spectra originating from protein vibrations.

The discriminating vector derived from SVM applied to the Raman spectra recorded using 532 nm as excitation wavelength shows positive signals within the CH stretching vibration region located at 2951 cm^{-1} and 2855 cm^{-1} . These bands can be assigned to shoulders of the CH signal due to lipid vibrations. A further signal located at 1481 cm^{-1} can be assigned to a DNA vibration and the signal located at 773 cm^{-1} originates from cytosine and uracil vibrations. The latter band, as well as its shoulder at 800 cm^{-1} assigned to an uracil ring stretching vibration, is utilized as a RNA marker. Protein bands appear in the discriminating vector at 1655, 1565, 1001, and 896 cm^{-1} . These findings correlate with the expected changes in cell physiology under ampicillin treatment and are consistent with findings in medical microbiology where the subinhibitory concentrations of antibiotics could be found to have a profound influence on physiology, gene expression, and secondary metabolite production [45–47].

The intense signal appearing at 1031 cm^{-1} and the minor signal at 1297 cm^{-1} are assigned to polysaccharide and phospholipid vibrations most likely associated with growth and formation of new cell membranes and walls. The negative signals of the discriminating vector correspond to the *E. coli* pDrive+amp spectra recorded from the challenged bacteria cultures. The signals at 1121 and 743 cm^{-1} originate from cytochrome *c* vibrations and indicate increased, stress-related respiration. The signals at 1220 and 977 cm^{-1} are assigned to protein vibrations, specifically

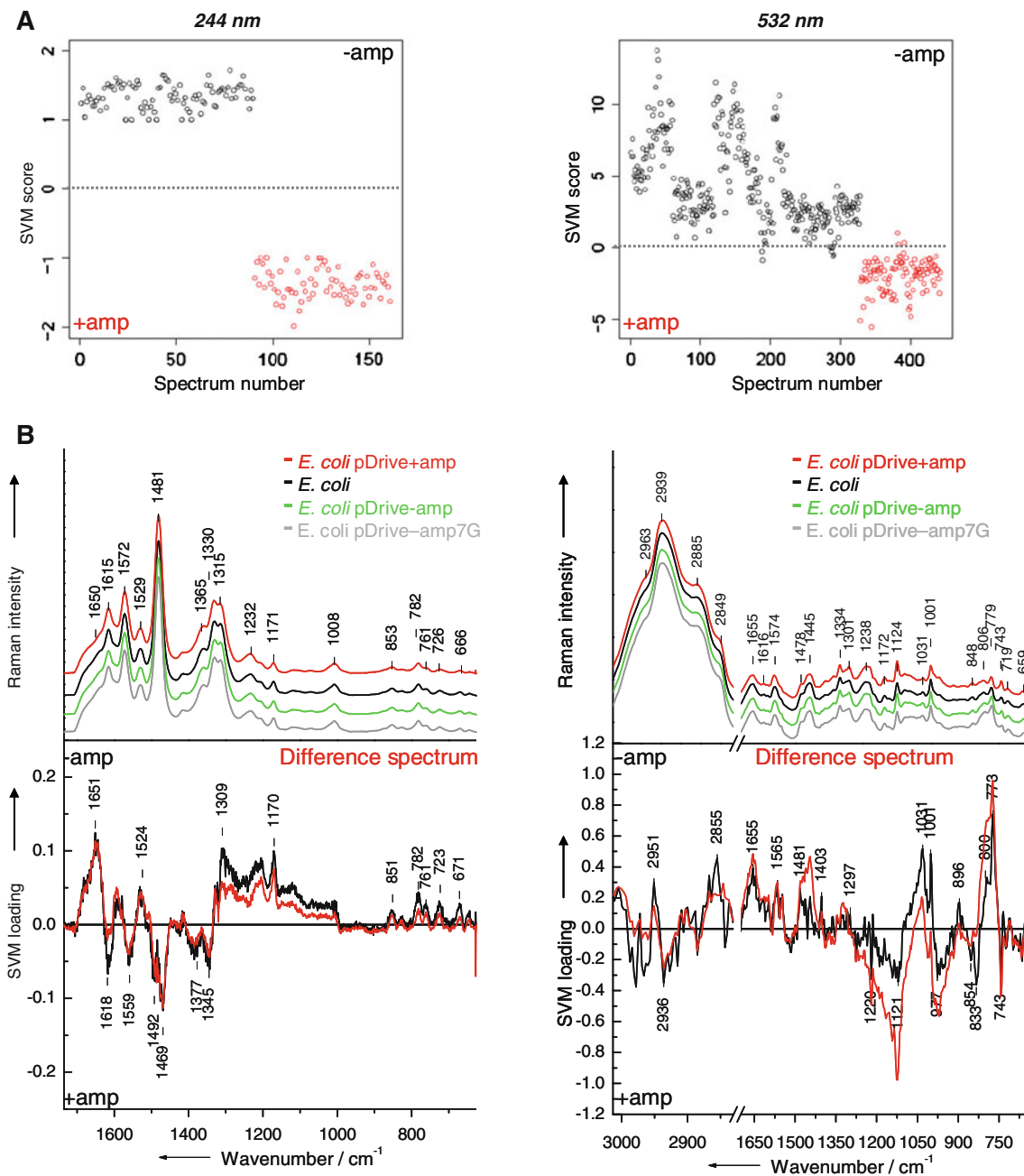


Fig. 4 Comparison of cultures with and without ampicillin treatment. **a** SVM scoreplot separating non-challenged bacteria (-amp, black: *E. coli*, *E. coli* pDrive-amp and *E. coli* pDrive-amp7G) from challenged *E. coli* pDrive+amp bacteria (+amp, red) utilizing Raman

spectra recorded using the excitation wavelengths of 244 nm (left) and 532 nm (right). **b** Raman spectra (preprocessed and averaged) of the four classes, the difference spectra of the class mean spectra and the discriminating SVM vectors (SVM loadings)

to amid III and C-C stretching of protein β -sheet structures pointing towards enhanced expression of proteins with higher β -sheet content, among them β -lactamase. However, the third marker band for protein β -sheet structures, expected at around 1670 cm⁻¹, cannot be identified in the discriminating vector. The intensity ratio of the two tyrosine vibrations located at 854 and 833 cm⁻¹ indicates higher content of buried tyrosine residues for *E. coli* pDrive+amp suggesting also new proteins expressed [48].

Concluding from the discriminating vectors of the Raman spectra recorded with the excitation wavelengths of 244 and 532 nm, the non-challenged *E. coli* cultures exhibit relatively higher DNA, RNA, lipid and polysaccharide content. The ampicillin-treated transformed cultures feature increased content of β -sheet structures with higher numbers of buried tyrosine residues and a higher cytochrome *c* content. Cytochrome, as an element of the respiration chain, is present in higher concentrations in the cells of the challenged

Table 2 SVM prediction of Raman spectra recorded using 244 nm as excitation wavelength

A		Challenged biological replicates													
Identified as		1	2	3	4	5	6	7	8						
Non-challenged (FN)		0	0	0	0	0	0	0	0						
Challenged (TP)		4	7	3	3	18	15	14	7						
Identified accuracy (%) for each replicate		100	100	100	100	100	100	100	100						
Identified accuracy (%) for the challenged class		100													
B		Non-challenged biological replicates													
Identified as		1	2	3	4	5	6	7	8	9	10	11	12	13	14
Non-challenged (TP)		8	6	10	3	8	3	4	8	6	6	7	8	5	5
Challenged (FN)		0	0	0	0	0	0	0	0	0	0	0	0	0	0
Identified accuracy (%) for each replicate		100	100	100	100	100	100	100	100	100	100	100	100	100	100
Identified accuracy (%) for the challenged class		100													

Independent biological replicates incubated under challenged conditions (A) and non-challenged conditions (B) are identified. For each identification test, the number of correctly identified spectra is given as true positive (TP) and of incorrectly identified spectra is given as false negative (FN). For each individual dataset (biological replicate) the identification accuracy (correctly identified spectra versus all spectra of the dataset) is given, as well as, the determined averaged identification accuracy for the challenged (A) and non-challenged class (B)

cultures. Additionally, the Raman spectroscopic measurements revealed the impact of the antibiotic agent on the overall protein composition especially concerning the secondary structure, e.g., due to β -lactamase expression.

Identification of independent cultural replicates within the challenged and non-challenged classes For the Raman spectroscopic classifications that have been discussed above,

several independent cultures were included for each class (*E. coli*, pDrive-amp, pDrive-amp7G and pDrive+amp). The four different bacterial classes contain each 5 to 14 biologically independent replicates incubated in different batches, and therefore, represent independent datasets. The identification accuracy will be determined for the challenged (+amp) and non-challenged (-amp) bacterial classes for the spectra recorded using the 244 nm (Table 2) and 532 nm

Table 3 SVM prediction of Raman spectra recorded using 532 nm as excitation wavelength

A		Challenged biological replicates												
Identified as		1	2	3	4	5								
Non-challenged (FN)		0	0	8	0	0								
Challenged (TP)		13	26	19	22	27								
Identified accuracy (%) for each replicate		100	100	70.4	100	100								
Identified accuracy (%) for the challenged class		94.1±13.3												
B		Non-challenged biological replicates												
Identified as		1	2	3	4	5	6	7	8	9	10	11	22	13
Non-challenged (TP)		13	43	28	30	23	26	19	12	13	38	29	6	30
Challenged (FN)		0	0	1	0	0	0	4	1	0	0	0	8	0
Identified accuracy (%) for each replicate		100	100	96.6	100	100	100	82.6	92.3	100	100	100	42.9	100
Identified accuracy (%) for the challenged class		93.0±16.0												

Independent biological replicates incubated under challenged conditions (A) and non-challenged conditions (B) are identified. For each identification test, the number of correctly identified spectra is given as true positive (TP) and of incorrectly identified spectra is given as false negative (FN). For each individual dataset (biological replicate) the identification accuracy (correctly identified spectra versus all spectra of the dataset) is given, as well as, the determined averaged identification accuracy for the challenged (A) and non-challenged class (B)

(Table 3) excitation wavelengths. For this experiment, the spectra of one of the individual biological replicates are removed from the dataset and the SVM model is trained. Then, the spectra of the unknown biological replicates are identified. The correctly (true positive) and incorrectly (false negative) identified number of spectra are summarized for each biological replicate of the challenged class in the sub-table A and of the non-challenged class in sub-table B for both excitation wavelengths. The identification accuracies defining the correctly identified spectra per dataset are determined for each biological replicate. The identification accuracies deriving from the individual biological replicates, which belong either to the challenged or non-challenged class, are averaged to specify the identification accuracies for both, the challenged and non-challenged class. The identification of spectra recorded using 244 nm as the excitation wavelength results in accuracies of 100% for all the eight independent biological replicates in the challenged class (Table 2A) and for the 14 independent biological replicates in the non-challenged class (Table 2B). If the excitation wavelength is 532 nm, the Raman spectra deriving from five independent biological replicates of the challenged class are correctly identified with $94.1 \pm 13.3\%$ (Table 3A). Concerning the identification of the 13 independent biological replicates of the non-challenged class, the identification accuracy results in $93.0 \pm 16.0\%$ (Table 3B).

Summary

Raman spectroscopy is feasible to classify *E. coli*, pDrive-amp, pDrive+amp and pDrive-amp7G spectra of the model strain excited at 244 and 532 nm revealing different separation features for the two excitation wavelengths. The classification applying both Raman excitation wavelengths results in the separation of the *E. coli* and pDrive-amp cultures due to the difference in the DNA content. Here, SVM was used to discuss two-class separation because the best classification accuracies were accomplished. However, the excitation at 532 nm presents additional characteristics related to the physiological state of the bacteria. The *E. coli* cultures exhibit higher cytochrome content, whereas the *E. coli* pDrive-amp cultures show higher lipid and RNA content.

LDA was applied to visualize the multi-class problem by comparing all four cultures with each other, including the ampicillin-challenged and non-challenged cultures. The gradual lower content of plasmid, originating from previous plasmid down regulation or a mixed culture, is reflected differently in the UVR spectra compared to spectra recorded using the excitation wavelength of 532 nm. For both excitation wavelengths, the cultures which have minimized plasmid content (*E. coli* pDrive-amp7G) are

very similar to the pDrive-amp cultures. However, this fact is even more pronounced for the spectra recorded with 532 nm as excitation wavelengths.

The transformed cultures, which are challenged by ampicillin supplement, separate clearly from the cultures without ampicillin treatment. The separation is based on vibrational changes exerted by a different protein secondary structure, variations in DNA/RNA moieties and increased cytochrome content of the challenged cultures. The predictions of independent biological replicates result in satisfying class accuracies for the spectra recorded with both excitation wavelengths.

Here, we have demonstrated that Raman spectroscopy is capable to identify spectral differences of bacterial cultures containing plasmids and those without plasmids. In addition, ampicillin-challenged and non-challenged bacteria of the model strain *E. coli* DH5 α are classified and identified. Distinct spectral features were identified correlating to cell constituents, which are responsible for the separation. Further studies concerning more strains and species should be carried out. These experiments could possibly be extended to other resistances like, e.g., heavy metal or organic pollutant resistance factors in addition to the clinical approaches for antibiotic resistance determination.

For further investigation, Raman spectroscopy offers the possibility of single cell measurements. Therefore, time-consuming cultivation as required in microbiological procedures can be omitted, when bacteria are characterized due to plasmid content and resistances. Within this study, the application of single cell measurement is constricted by the undefined plasmid content of the individual cells.

Acknowledgment We gratefully acknowledge financial support from the Deutsche Forschungsgemeinschaft (Graduiertenkolleg GK 1257 "Alteration and element mobility at the microbe-mineral interface" in the frame of the Jena School of Microbial Communication and Po563/7-2).

References

- Schlegel GH (1992) Allgemeine Mikrobiologie, 7th edn. Thieme, Stuttgart
- Ream W (1989) Annu Rev Phytopathol 27:583–618
- Lilley AK, Bailey MJ (1997) Appl Environ Microbiol 63:1577–1583
- Wang RF, Cao WW, Cerniglia CEJ (1997) Appl Microbiol 83:727–736
- Maquelin K, Choo-Smith LP, Kirschner C, Ngo-Thi NA, Naumann D, Puppels GJ (2002) Handbook of Vibrational Spectroscopy. In: Chalmers JM, Griffiths PR (eds), vol 5. Wiley, Chichester, pp 3308
- Sadovskaya I, Vinogradov E, Li J, Jabbouri S (2004) Carbohydr Res 339:1467–1473
- Hahn H, Falke D, Kaufmann SHE, Ullmann U (2005) Medizinische Mikrobiologie und Infektiologie, 5th edn. Springer, Heidelberg
- Riou JY, Caugant DA, Selander RK, Poolman JT, Guibourdenche M, Collatz E (1991) Eur J Clin Microbiol Infect Dis 10:405–409

9. Kharlamenko VI, Kiyashko SI, Imbs AB, Vyshkvartzev DI (2001) *Mar Ecol Prog Ser* 220:103–117
10. Kilic NK, Stensballe A, Otzen DE, Doenmez G. *Bioresour Technol* 101:2134–2140
11. Baena JR, Lendl B (2004) *Curr Opin Chem Biol* 8:534–539
12. Schrader B, Dippel B, Erb I, Keller S, Lochte T, Schulz H, Tatsch E, Wessel SJ (1999) *Mol Struct* 480–481:21–32
13. Schweitzer-Stenner RJ (2005) *Raman Spectrosc* 36:276–278
14. Walter A, Erdmann S, Bocklitz T, Jung E-M, Vogler N, Akimov D, Dietzek B, Rösch P, Kothe E, Popp J (2010) *Analyst* 135:908–917
15. Neugebauer U, Schmid U, Baumann K, Ziebuhr W, Kozitskaya S, Deckert V, Schmitt M, Popp J (2007) *Chemphyschem* 8:124–137
16. Stöckel S, Meisel S, Böhme R, Elschner M, Rösch P, Popp JJ (2009) *Raman Spectrosc* 40:1469–1477
17. Tripathi A, Jabbour RE, Treado PJ, Neiss JH, Nelson MP, Jensen JL, Snyder AP (2008) *Appl Spectrosc* 62:1–9
18. Schuster KC, Urlaub E, Gapes JRJ (2000) *Microbiol Meth* 42:29–38
19. Schuster KC, Reese I, Urlaub E, Gapes JR, Lendl B (2000) *Anal Chem* 72:5529–5534
20. Rösch P, Harz M, Schmitt M, Peschke K-D, Ronneberger O, Burkhardt H, Motzkus H-W, Lankers M, Hofer S, Thiele H, Popp J (2005) *Appl Environ Microbiol* 71:1626–1637
21. Krause M, Radt B, Rösch P, Popp JJ (2007) *Raman Spectrosc* 38:369–372
22. Harz M, Kiehntopf M, Stöckel S, Rösch P, Straube E, Deufel T, Popp J (2009) *J Biophotonics* 2:70–80
23. Tarcea N, Harz M, Rösch P, Frosch T, Schmitt M, Thiele H, Hochleitner R, Popp J (2007) *Spectrochim Acta A* 68A:1029–1035
24. Gaus K, Rösch P, Petry R, Peschke KD, Ronneberger O, Burkhardt H, Baumann K, Popp J (2006) *Biopolymers* 82:286–290
25. Neugebauer U, Schmid U, Baumann K, Ziebuhr W, Kozitskaya S, Holzgrave U, Schmitt M, Popp JJ (2007) *Phys Chem* 111:2898–2906
26. Lopez-Diez EC, Winder CL, Ashton L, Currie F, Goodacre R (2005) *Anal Chem* 77:2901–2906
27. Maquelin K, Kirschner C, Choo-Smith LP, van den Braak N, Endtz HP, Naumann D, Puppels GJJ (2002) *Microbiol Meth* 51:255–271
28. Moritz TJ, Taylor DS, Polage CR, Krol DM, Lane SM, Chan JW (2010) *Anal Chem* 82:2703–2710
29. Serban D, Benevides JM, Thomas GJ Jr (2002) *Biochemistry* 41:847–853
30. Taylor RG, Walker DC, McInnes RR (1993) *Nucleic Acids Res* 21:1677–1678
31. Sambrook JF, Russell DW (Eds) (2000) *Molecular cloning: a laboratory manual*, third edition
32. The R Development Core Team (2009) *R: a Language and Environment for Statistical Computing*, R Foundation for Statistical Computing, Vienna, Austria ISBN 3-900051-07-0
33. Ryan CG, Clayton E, Griffin WL, Sie SH, Cousens DR (1988) *Nucl Instrum Methods Phys Res Sect B* B34:396–402
34. Fearn T (2002) *Handbook of Vibrational Spectroscopy*. In: Chalmers JM, Griffiths PR(eds) Wiley, Chichester, vol 3, pp 2086
35. Cortes C, Vapnik V (1995) *Mach Learn* 20:273–297
36. Ivanciu O, Lipkowitz KB, Cundari TR (eds) (2007) *Wiley-VCH*, Wiley. pp 291–400
37. Chang CC, Lin CJ (2001) *LIBSVM: a library for support vector machines*
38. Movasaghi Z, Rehman S, Rehman IU (2007) *Appl Spectrosc Rev* 42:493–541
39. Harz M, Claus RA, Bockmeyer CL, Baum M, Rösch P, Kentouche K, Daigner HP, Popp J (2006) *Biopolymers* 82:317–324
40. Kitagawa T, Kyogoku Y, Iizuka T, Ikeda-Saito M, Yamanaka TJ (1975) *Biochem* 78:719–728
41. Nelson WH, Manoharan R, Sperry JF (1991) *Appl Spectrosc Rev* 27:67–124
42. Frushour BG, Koenig JL (1974) *Biopolymers* 13:455–474
43. Benveniste R, Davies J (1973) *Annu Rev Biochem* 42:471–506
44. Rimpler H (1999) In *Biogene Arzneistoffe*; Deutscher Apotheker Verlag, Stuttgart
45. Chifiriuc M-C, Ditu L-M, Banu O, Bleotu C, Dracea O, Bucur M, Larion C, Israil Anca M, Lazar V (2009) *Roum Arch Microbiol Immunol* 68:27–33
46. Deneve C, Bouttier S, Dupuy B, Barbut F, Collignon A, Janoir C (2009) *Antimicrob Agents Chemother* 53:5155–5162
47. Lopez E, Blazquez J (2009) *Antimicrob Agents Chemother* 53:3411–3415
48. Craig WS, Gaber BPJ (1977) *Am Chem Soc* 99:4130–4134